

Chemo-immune synergetic therapy of esophageal carcinoma: trastuzumab modified, cisplatin and fluorouracil co-delivered lipid-polymer hybrid nanoparticles

Qingxia Fu^a, Jiancheng Wang^b and Hong Liu^c

^aDepartment of Pharmacy, Linyi People's Hospital, Linyi, PR China; ^bDepartment of Traditional Chinese Medicine, Shandong Linyi Inspection and Testing Center, Linyi, PR China; ^cDepartment of Infectious Diseases, Linyi People's Hospital, Linyi, PR China

ABSTRACT

Esophageal cancer is the sixth most common cause of cancer-related death worldwide. Peptide modified nanoparticles have been engineered as novel strategies to improve esophageal adenocarcinoma (EAC) therapy. This study aimed to develop a trastuzumab (TAB) modified system for the delivery of cisplatin (CIS) and fluoropyrimidine (5-FU). In the present study, CIS and 5-FU co-encapsulated lipid-polymer hybrid nanoparticles (CIS/5-FU LPHNs) were prepared. TAB was conjugated to the surface of CIS/5-FU LPHNs to achieve TAB decorated CIS/5-FU LPHNs (TAB-CIS/5-FU LPHNs). After the *in vitro* assessment, a subcutaneous model was used for the *in vivo* study. The mean diameter of LPHNs was around 100 nm, with higher encapsulation efficacy (EE) of about 90%. The LPHNs was stable and able to release drugs in sustained manners. 63.9% of cell uptake was achieved by TAB-CIS/5-FU LPHNs, with the best *in vivo* antitumor ability. The best synergistic effect with the lowest CI value (0.68) was achieved at the ratio of 1/1, which was determined for the dosage of drugs in the LPHNs preparation. TAB-CIS/5-FU LPHNs provide a new strategy for synergistic treating of EAC with higher efficacy and reduced side effects, introducing this system as a candidate for EAC therapy.

ARTICLE HISTORY

Received 26 August 2020
Revised 12 October 2020
Accepted 12 October 2020

KEYWORDS

Esophageal adenocarcinoma; combination therapy; cisplatin; fluorouracil; targeted therapy



Introduction

Esophageal cancer is the sixth most common cause of cancer-related death worldwide (Jemal et al., 2011). The incidence and types of esophageal cancer (two types: squamous cell carcinoma and adenocarcinoma) are different in different regions (Siewert & Ott, 2007). High-prevalence areas include Asia, southern and eastern Africa, etc. (Pickens & Orringer, 2003; Bosetti et al., 2008). Meanwhile, because of its incidence has risen more steeply, esophageal adenocarcinoma (EAC) has become a major public health issue, especially in Western countries (Pohl & Welch, 2005; Lindblad et al., 2006). The strong risk factors for EAC include obesity, high body mass index, gastroesophageal reflux disease (GERD), and Barrett's esophagus. Therefore, with the improvement of people's living standard, the incidence and threat of EAC will continue to increase (Chow et al., 1995; Vaughan et al., 1995; Cossentino & Wong, 2003). Moreover, its prognosis is still very poor and 5-year survival rate is below 20%. Chemotherapy is the recommended choice for patients with locally advanced or metastatic EAC.

Combination chemotherapy (cisplatin (CIS) and fluorouracil) is the most investigated and most commonly applied regimen for patients with esophageal cancer (Ychou et al., 2011). Based on the results of ToGA trial, the guidelines

recommend the combination of trastuzumab (TAB) plus first-line chemotherapy (category 1 for combination with CIS and fluoropyrimidine) for patients with HER2-overexpressing adenocarcinoma (Bang et al., 2010). The principles of targeted therapy (TAB) plus CIS and fluoropyrimidine (5-FU) are as follows: (1) CIS and 5-Fu are the chemotherapy regimen, and CIS has demonstrated synergistic anti-esophageal cancer activity when combined with 5-Fu (Jung et al., 2013); (2) TAB, a HER2 targeted therapeutic antibody, in combination with chemotherapeutic agents, can bind to HER2 receptors on target cancer cells such as HER2-overexpressing EAC (Moelans et al., 2010; Schoppmann et al., 2010); (3) in clinic, patients are administrated with TAB, CIS, and 5-FU via intravenous (i.v.) infusion at the same time; (4) the treatment plan is repeated every 2 weeks with several cycles to achieve therapeutic efficacy. Although this combination has produced encouraging results and improved survival, some severe obstacles like multi-drug resistance, side effects, and short efficacy have hindered the application in the clinic.

Recently, multifunctional nanocarriers have been engineered as novel strategies to improve EAC therapy, which include liposomes for chemo-radiotherapy, peptide modified nanoparticles combined NP platform and confocal laser endomicroscopy, and chitosan-coated gold/gold sulfide nanoparticles (Li et al., 2013; Chang et al., 2015; Dassie et al.,

CONTACT Hong Liu  hongliulph@aliyun.com  Department of Infectious Diseases, East Medical District of Linyi People's Hospital, No. 233 Fenghuang Street, Linyi 276000, Shandong Province, PR China

© 2020 The Author(s). Published by Informa UK Limited, trading as Taylor & Francis Group.

This is an Open Access article distributed under the terms of the Creative Commons Attribution-NonCommercial License (<http://creativecommons.org/licenses/by-nc/4.0/>), which permits unrestricted non-commercial use, distribution, and reproduction in any medium, provided the original work is properly cited.

2015). In our study, anti-HER2 antibody conjugated nanoparticles, an attractive approach for the treatment of HER2-positive cancer, were designed for targeted, chemo-immune synergetic therapy of EAC (Niza et al., 2019; Kim et al., 2020; Rodalleg et al., 2020).

In the present study, CIS and 5-FU co-encapsulated lipid-polymer hybrid nanoparticles (CIS/5-FU LPHNs) were prepared. TAB was conjugated to the surface of CIS/5-FU LPHNs to achieve TAB decorated CIS/5-FU LPHNs (TAB-CIS/5-FU LPHNs).

Materials and methods

Materials

DSPE-PEG-COOH was purchased from Ponsure Biological (Shanghai, China). CIS, 5-FU, soy phosphatidylcholine (SPC), 1-ethyl-3-(3-dimethylaminopropyl) carbodiimide (EDC), N-hydroxysuccinimide (NHS), Dulbecco's Modified Eagle's Medium (DMEM), and coumarin-6 (C-6) were purchased from Sigma-Aldrich (St. Louis, MO). RPMI Medium 1640, fetal bovine serum (FBS), and 3-(4,5-dimethyl-2-thiazolyl)-2,5-diphenyl-2-H-tetrazolium bromide (MTT) were purchased from Invitrogen Corporation (Carlsbad, CA). All other chemicals and reagents were of analytical grade or high-performance liquid chromatography (HPLC) grade and used without further purification.

Preparation of CIS/5-FU LPHNs

CIS/5-FU LPHNs (Figure 1) were prepared using a solvent displacement method with some modifications (Silva et al., 2015). CIS (20 mg), 5-FU (different ratio to CIS), and PCL (100 mg) were dissolved in acetone (20 mL) (mixture 1). DSPE-PEG-COOH (50 mg) and SPC (50 mg) were dispersed in deionized water (80 mL), warmed to about 60 °C and then added dropwise to the mixture 1 stirred at a speed of 300 round per minute (rpm). The dispersion was further stirred overnight to remove the residual organic solvent. Single drug loaded and blank LPHNs (CIS LPHNs, 5-FU LPHNs, and LPHNs) were prepared by the same procedure using CIS or 5-FU only. All LPHNs were isolated by centrifugation at 10,000×g for 30 min at 4 °C to remove unbound drug.

Preparation of TAB-CIS/5-FU LPHNs

The TAB was chemically conjugated to CIS/5-FU LPHNs by amido linkage (Niza et al., 2019). Briefly, TAB (20 mg) were dissolved in PBS (5 mL, pH 7.4), followed by the addition of EDC (40 mg) and NHS (10 mg). CIS/5-FU LPHNs PBS suspension (2 mL) was added to TAB solution and stirred at 300 rpm for 10 h. The suspension was centrifuged at 10,000×g for 30 min at 4 °C to remove the excess of EDC and NHS. TAB-CIS/5-FU LPHNs (Figure 1), CIS/5-FU LPHNs, CIS LPHNs, and 5-FU LPHNs were stored at 2–8 °C before use.

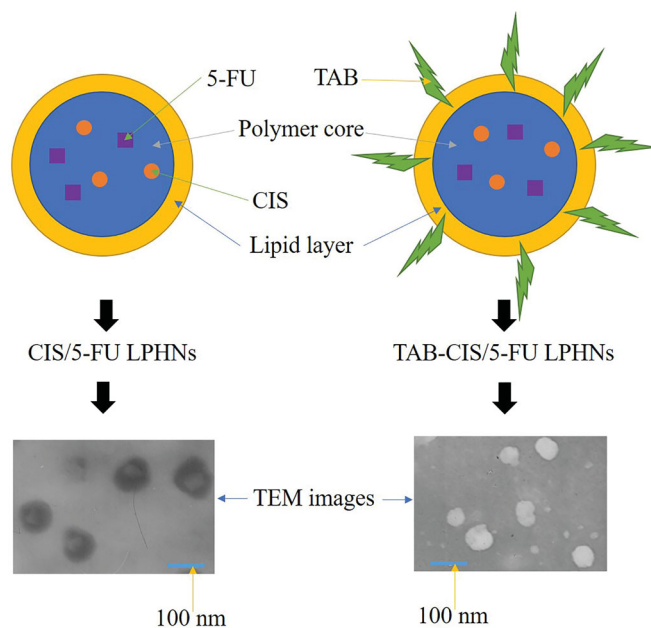


Figure 1. Scheme graphs and TEM images of CIS/5-FU LPHNs and TAB-CIS/5-FU.

Characterization of LPHNs

TAB conjugation of TAB-CIS/5-FU LPHNs was evaluated by measuring the absorbance of the eluates of TAB-CIS/5-FU LPHNs and free TAB using an enhanced BCA protein assay kit at 562 nm (Guo et al., 2019).

The shape, morphology, and size of TAB-CIS/5-FU LPHNs and CIS/5-FU LPHNs were characterized by transmission electron microscopy (TEM, JEM-1200EX, JEOL, Tokyo, Japan) (Çedrowska et al., 2020). The hydrodynamic diameter and zeta potential of LPHNs were determined by dynamic light scattering (Zetasizer Nano ZS DLS, Malvern, UK).

Drug loading, encapsulation efficacy, and stability of LPHNs

The CIS drug loading (DL) and encapsulation efficacy (EE) were measured using ICP-MS (Yang et al., 2016). CIS loaded LPHNs were digested in 70% HNO₃ and diluted in water to a final acid content of 2%. The CIS concentration was determined according to the standard curve derived from a series of CIS dilutions. The 5-FU DL and EE were analyzed by HPLC using a Waters column with a guard column pumped at a flow rate of 0.5 mL/min (Fernandes et al., 2019). The mobile phase was composed of acetonitrile and water (5:95, v/v) and the volume of sample injected was 10 µL. The detection wavelength was 265 nm. The stability of LPHNs was evaluated during 3 months of storage at 2–8 °C by assessing the particle size, and EE (Pang et al., 2020).

In vitro release of LPHNs

In vitro drug release behaviors of LPHNs were determined by dialysis method (Wang et al., 2015). Drugs loaded LPHNs were reconstituted in PBS (5 mL, pH 7.4) in dialysis bags (MWCO: 20 kDa) that were placed in the same PBS (30 mL,

pH 7.4) and stirred at a speed of 220 g (37 °C). At determined time points, the dialysate (100 µL) was collected and the dialysate replenished with the same amount of fresh PBS. The concentration of the released CIS and 5-FU was tested using the methods in the above section.

Cells and animals

Human esophageal cancer cell line (adenocarcinoma, BE-3) was obtained from American Type Culture Collection (Manassas, VA) and maintained in DMEM. Xenografts of esophageal cancer Balb/c-nude mice (4 weeks old) were purchased from Laboratory Animal Center of Shandong University (Ji'nan, China) and maintained in plastic cages in an SPF-grade animal room with access to food and water *ad libitum*. BE-3 cells were implanted in nude mice by subcutaneous injections of cells (5×10^6 in 100 µL) into the right hind limb to achieve EAC-bearing xenograft. All animal experiments comply with U. K. Animals Act (1986) and associated guidelines (2010/63/EU) for animal experiments and were approved by the Animal Ethics Committee of Linyi People's Hospital.

Cell uptake of LPHNs

Cell uptake extent of LPHNs was measured by encapsulating C-6 as an indicator (Bian & Guo, 2020). C-6 encapsulated TAB-CIS/5-FU LPHNs and CIS/5-FU LPHNs were added to BE-3 cells and incubated for 1 h. Cells were then washed with PBS (1 mL) and photographed by fluorescence microscopy. A BD FACSCalibur flow cytometer was applied to quantitate the cell uptake efficiency of LPHNs.

Cytotoxicity of LPHNs

BE-3 cells viability was evaluated by MTT assay to evaluate the cytotoxicity of LPHNs (Yu et al., 2010). Cells were seeded into 96-well plates (1×10^4 cells/well). After incubation in a 5% CO₂ incubator at 37 °C for 24 h, the culture medium was replaced with of fresh DMEM (200 µL) containing various concentrations of the LPHNs or CIS and 5-FU mixed solution (CIS/5-FU) and incubated for an additional 24 h. MTT (5 mg/mL) was added to each well, and the plate was incubated for another 4 h. Then the medium was removed, and the crystals were dissolved in DMSO (100 µL). The absorbance at 570 nm was tested using a microplate reader. Untreated cells were applied as control.

Synergistic effect of LPHNs

The half-maximal inhibitory concentration (IC₅₀) values of CIS/5-FU LPHNs, CIS LPHNs, and 5-FU LPHNs were calculated by the results of BE-3 cells viability. The synergistic effect of LPHNs was evaluated by Chou and Talalay's method (Chou & Talalay, 1983). Combination index (CI) was calculated according to the IC₅₀ values: $CI = \frac{\text{the concentrations of CIS in CIS/5-FU LPHNs}}{\text{IC}_{50} \text{ value of CIS}} + \frac{\text{the concentrations of 5-FU in CIS/5-FU LPHNs}}{\text{IC}_{50} \text{ value of 5-FU}}$. CI values larger than 1

represent antagonism, less than 1.0 indicate synergy, with values closer to zero representing increasing synergy.

In vivo antitumor ability and toxicity of LPHNs

When the tumor volume reached about 100 mm³, EAC-bearing xenograft were divided randomly into seven groups (10 mice per group) and treated with CIS/5-FU LPHNs, CIS LPHNs, 5-FU LPHNs, LPHNs, TAB-CIS/5-FU LPHNs (LPHNs contained 5 mg CIS and/or 5 mg 5-FU per g of mice), CIS/5-FU (contained 10 mg CIS and 10 mg 5-FU per g of mice), and 0.9% saline solution every three days through the tail vein (Chang et al., 2015). Tumor sizes were recorded before each injection using a caliper to monitor the tumor growth.

Toxicity was observed every three days by the changes in mouse weight and other indicators. Immunological toxicity was examined by counting the white blood cells (WBCs). Hematological toxicities representing the functions of liver and kidneys were measured by detecting the alanine aminotransferase (ALT) and creatinine (CRE).

Statistical analysis

Comparison of the two groups was performed using Student's *t*-test (SPSS Software, Chicago, IL). Multiple groups were compared by one-way ANOVA with Dunnett's post-test. The results are expressed as the mean ± standard deviation. A value of $p < .05$ was considered significant and $p < .01$ was considered highly significant.

Results

Characterization of LPHNs

The absorbance curves of TAB-CIS/5-FU LPHNs and free TAB are put together in Figure 2 for comparison. Free TAB showed one peak, which was also existed in the TAB-CIS/5-FU LPHNs absorbance curve. One of the two peaks in the curve of TAB-CIS/5-FU LPHNs is overlapped with the peak of TAB, illustrated the TAB conjugation on the LPHNs surface. TEM images of TAB-CIS/5-FU LPHNs and CIS/5-FU LPHNs are presented in Figure 1. TAB-CIS/5-FU LPHNs had one more dark coating on the particles than that of CIS/5-FU LPHNs, which could prove the successful TAB decoration on the other side. After decoration, the zeta potential of LPHNs decreased than that of CIS/5-FU LPHNs, this may be explained by the negative charge of TAB (Table 1). The mean diameter of LPHNs was around 100 nm, with higher EE of about 90%. The particle size, and EE exhibited negligible changes during 3 months of storage, which could demonstrate the stability of LPHNs.

In vitro release behavior

In vitro drug release behaviors of LPHNs are illustrated in Figure 3. TAB-CIS/5-FU LPHNs showed more sustained release pattern than their CIS/5-FU LPHNs counterparts, which may be influenced by the TAB on the surface of the particles. It

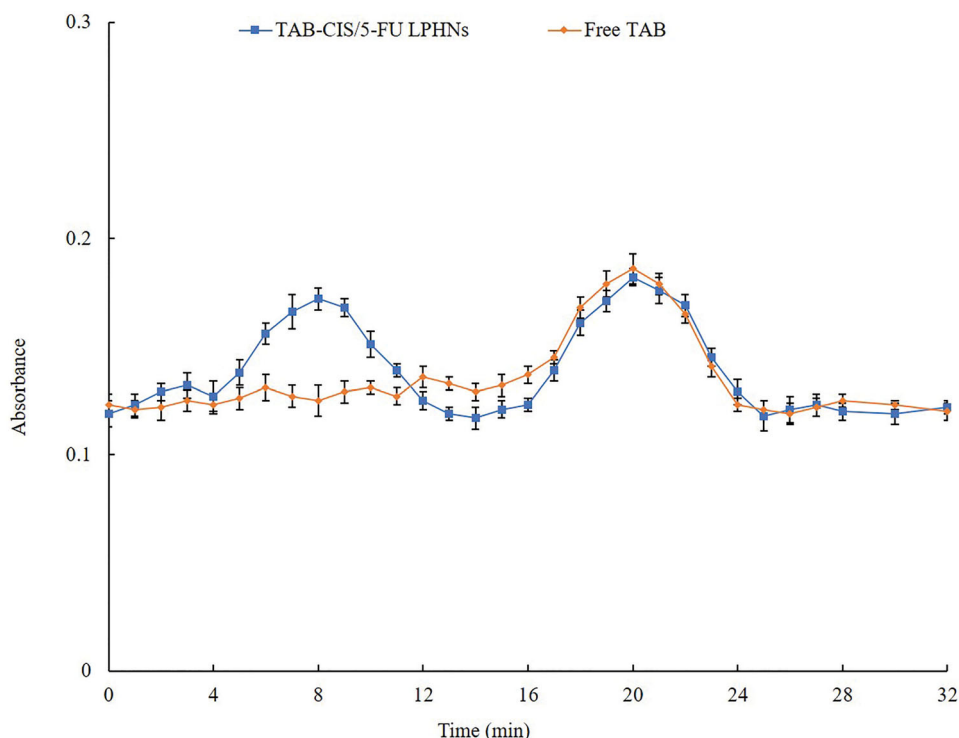


Figure 2. The absorbance curves of TAB-CIS/5-FU LPHNs and free TAB. Values represented as mean \pm standard deviation ($n = 10$).

Table 1. Physicochemical properties of nanoparticles.

Nanoparticles	Mean diameter (nm)	PDI	Zeta potential (mV)	EE of CIS (%)	EE of 5-FU (%)	DL of CIS (%)	DL of 5-FU (%)
CIS/5-FU LPHNs	101.9 \pm 4.8	0.15 \pm 0.2	13.6 \pm 1.5	90.1 \pm 2.8	89.5 \pm 3.2	5.9 \pm 0.5	4.1 \pm 0.6
CIS LPHNs	102.6 \pm 4.5	0.16 \pm 0.1	15.1 \pm 2.1	91.3 \pm 3.1	–	6.2 \pm 0.4	–
5-FU LPHNs	98.9 \pm 4.3	0.13 \pm 0.2	12.9 \pm 1.8	–	90.4 \pm 2.5	–	5.3 \pm 0.7
LPHNs	100.3 \pm 3.2	0.11 \pm 0.1	14.6 \pm 1.7	–	–	–	–
TAB-CIS/5-FU LPHNs	105.2 \pm 5.1	0.18 \pm 0.2	28.5 \pm 1.9	89.7 \pm 2.9	90.1 \pm 3.7	4.3 \pm 0.7	4.1 \pm 0.6

Values represented as mean \pm standard deviation ($n = 10$).

took 48 h for CIS to complete the release from CIS/5-FU LPHNs, while the time of CIS to release from TAB-CIS/5-FU LPHNs was 60 h. The same behaviors were found on the 5-FU release profiles.

Cell uptake efficiency

Cell uptake efficiency of TAB-CIS/5-FU LPHNs and TAB-CIS/5-FU LPHNs are of significant differences as shown in the fluorescence images (Figure 4(A)). Figure 4(B) exhibits that 63.9% of cell uptake was achieved by TAB-CIS/5-FU LPHNs, which was higher than that of CIS/5-FU LPHNs (31.6%) ($p < .05$). Higher uptake capacity may increase the cytotoxicity of the system which was evaluated in the next section.

In vitro cytotoxicity and synergistic effect

Blank LPHNs showed negligible cytotoxicity, while drugs contained formulas exhibited dose-dependent cell inhibition effects (Figure 5). Free CIS/5-FU exhibited remarkable higher cytotoxicity than the control ($p < .05$). CIS/5-FU LPHNs inhibited the tumor cell growth better than CIS/5-FU ($p < .05$). TAB-CIS/5-FU LPHNs illustrated the most prominent cytotoxicity, which is more cytotoxic than CIS/5-FU LPHNs ($p < .05$). To evaluate the synergistic effect of the dual drugs loaded

LPHNs, CI values were calculated due to different CIS to 5-FU ratios. When CIS to 5-FU ratios were between 5/1 and 1/5, dual drugs loaded CIS/5-FU LPHNs showed synergy effects (Table 2). The best synergistic effect with the lowest CI value (0.68) was achieved at the ratio of 1/1, which was determined for the dosage of drugs in the LPHNs preparation.

In vivo antitumor ability and systemic toxicity

In vivo antitumor ability of TAB-CIS/5-FU LPHNs was significantly better than that of CIS/5-FU LPHNs and other formulas (Figure 6(A), $p < .05$). The combination of CIS and 5-FU in CIS/5-FU LPHNs inhibited tumor growth greater than single drug contained CIS LPHNs and 5-FU LPHNs ($p < .05$). No obvious body weight change was found in LPHNs groups (Figure 6(B)), indicating there are no serious systemic toxicity. However, remarkable reduction in weight was found in free CIS/5-FU group, which is also found an increase of CRE (Table 3). The WBC and ALT values of all the samples tested are in the normal range (Table 3).

Discussion

LPHNs are new-generation core-shell nanostructures with a polymer core enveloped by a lipid layer (Wang et al., 2019).

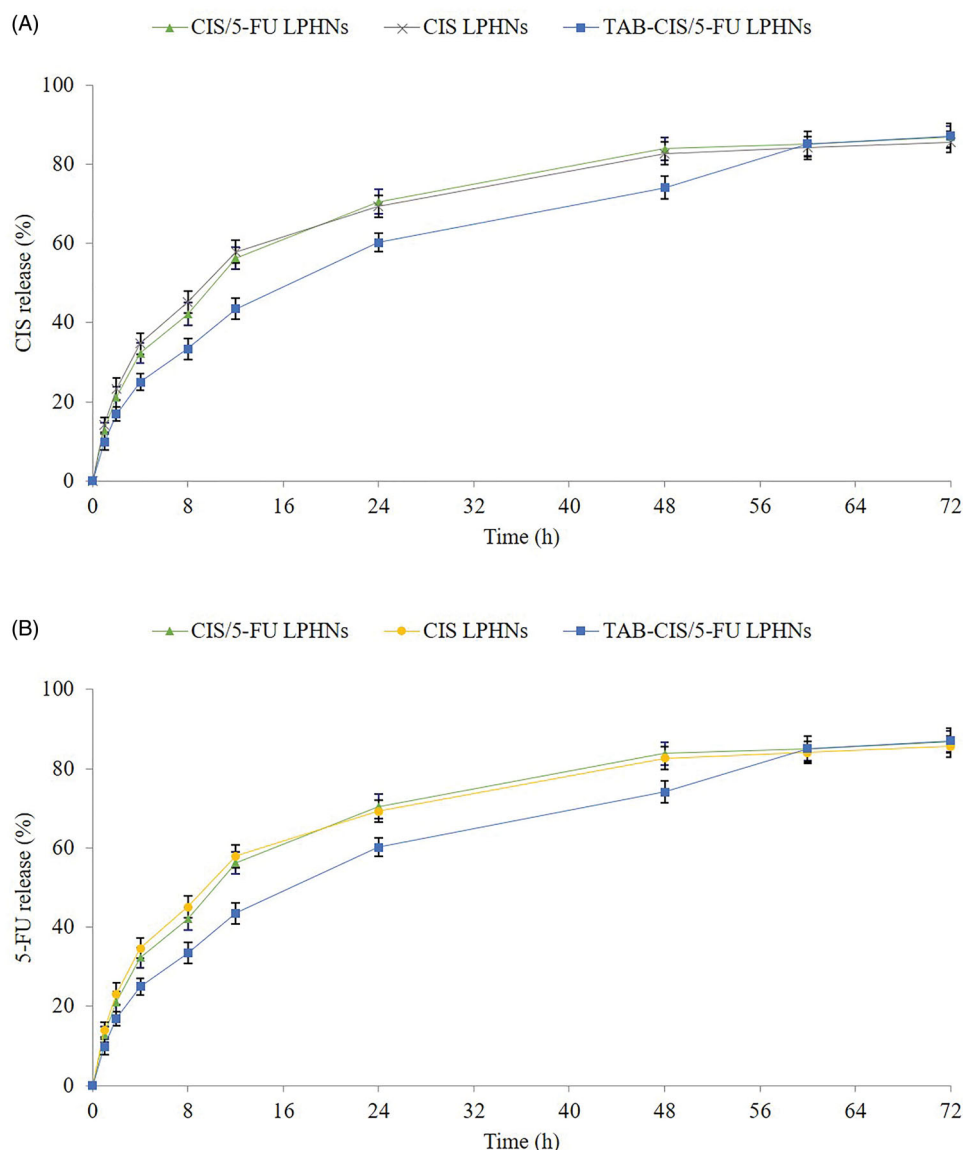


Figure 3. *In vitro* CIS (A) and 5-FU (B) release behaviors of LPHNs. Values are expressed as the mean \pm standard deviation. Values represented as mean \pm standard deviation ($n = 10$).

It was reported that LPHNs with uniform particle distribution and sizes between 100 and 200 nm (Thanki et al., 2019). The surface morphology of TAB-CIS/5-FU LPHNs in this study showed uniform particles with dark coating on the surface compared with CIS/5-FU LPHNs, this may prove the existence of TAB on the surface. The efficacy and safety of TAB were proved for patients with HER2-positive EAC, due to the HER2 receptors overexpressed on EAC cells (Soularue et al., 2015; Doi et al., 2017). In the present study, TAB was conjugated onto CIS/5-FU LPHNs surface through amido linkage.

The core-shell structured LPHNs may affect the release behavior of the systems (Zhang et al., 2017). The surface modifier is reported as a molecular fence that helps to retain the drugs inside the particles (Miao et al., 2014). The sustained release manner of TAB-CIS/5-FU LPHNs could protect the drugs for a relatively longer time from being degraded in the circulation system, prevent premature drug release prior to reaching the tumor sites and thus may perform persistent therapeutic effect.

The therapeutic effects of the drug loaded NPs would depend on the uptake of the particles by cancer cells (Hong et al., 2019). Coumarin 6 (C-6) is a fluorescent probe, which was used to represent the particles internalized the cells (Makwana et al., 2011). TAB-CIS/5-FU LPHNs showed higher uptake than that of CIS/5-FU LPHNs, which revealed that the LBL NPs had excellent ability to enter cancer cells. This characteristic could improve the therapeutic efficacy of the system. These findings were in accordance with the research carried by Ruan et al, who argued that substance P modified nanoparticles achieved higher uptake efficiency than non-modified nanoparticles (Ruan et al., 2018). Their peptide could act with the NK-1 receptors on tumor cells, resulting in higher cellular uptake results.

Significant cytotoxic actions were expected for a nanoparticle system. The higher cytotoxicity of TAB-CIS/5-FU LPHNs than CIS/5-FU LPHNs could be explained by the cellular uptake results (Oh et al., 2013). The use of multiple drugs in combination may present, synergism, additive, or antagonism

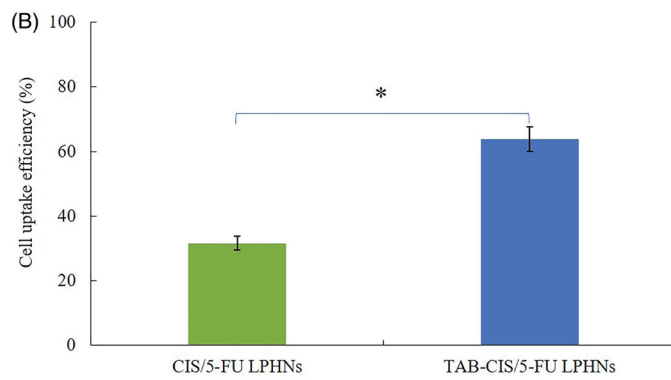
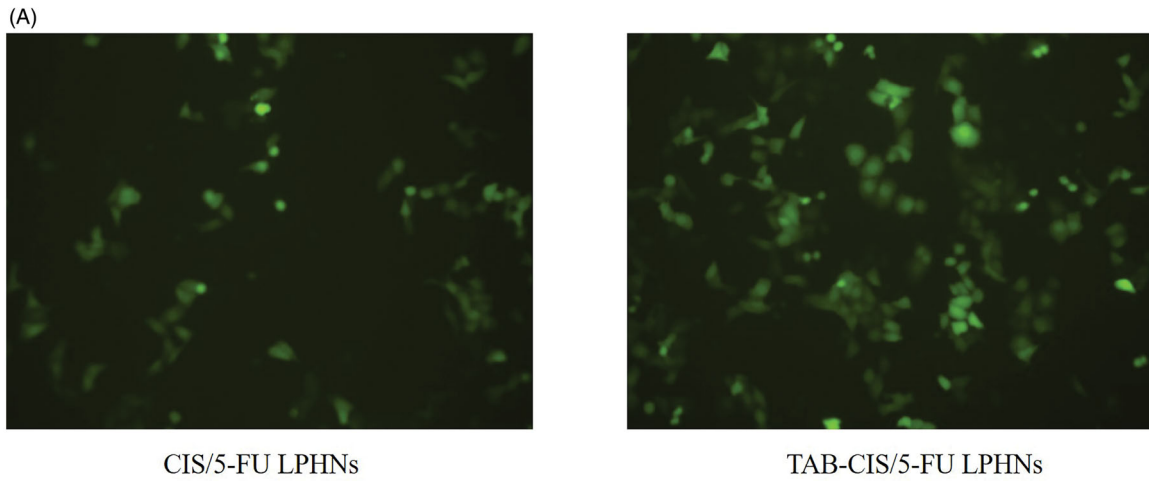


Figure 4. Cell uptake efficiency of TAB-CIS/5-FU LPHNs and TAB-CIS/5-FU LPHNs photographed by fluorescence microscopy (A) and quantitated through a flow cytometer (B). Values represented as mean \pm standard deviation ($n = 10$).

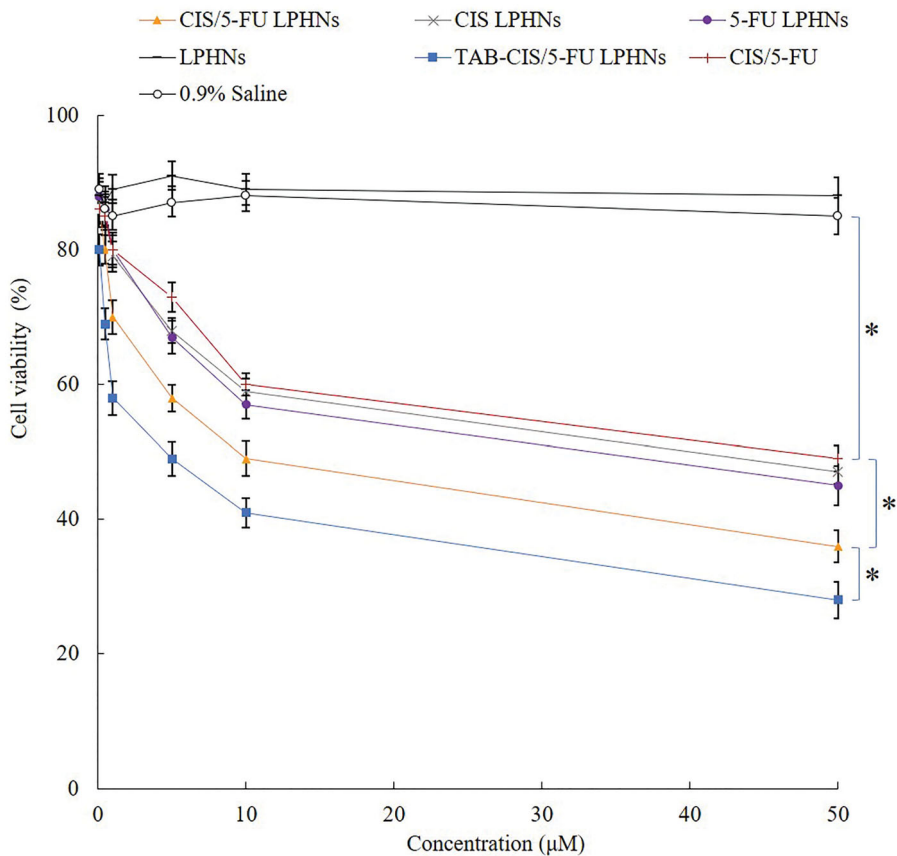


Figure 5. The cytotoxicity of LPHNs evaluated on BE-3 cells by MTT assay. Values represented as mean \pm standard deviation ($n = 10$).

outcomes (Cao et al., 2019). CI values were applied to evaluate the possible effect of the drug combinations. All CI values of CIS/5-FU LPHNs were less than 1.0, indicating the tested combination ratios tested all have synergistic effects. The smaller the CI value was, the stronger the synergistic efficacy. The best synergism effect was recorded as the IC value of 0.68 at the CIS to 5-FU ratio of 1:1. This result determined the amounts of drugs used in LPHNs preparation.

It has been reported that rational drug scheduling plays an important role in combination cancer therapy, which may result in optimized therapeutic effect (Mukthavaram et al., 2013). Owing to the high degree of potency *in vitro*, LPHNs were expected to exert useful therapeutic effects even with lower concentrations of drugs (Li et al., 2014). CIS/5-FU LPHNs inhibited tumor growth greater than free CIS/5-FU with lower drug contents. Ligands modified LPHNs were proved to exhibit the most potent anti-tumor activity among all the groups related to the targeted ability of the ligands (Duan & Liu, 2018). The same phenomenon was found in this section that TAB-CIS/5-FU LPHNs inhibitor the *in vivo* tumor growth better than that of CIS/5-FU LPHNs and other formulas. This was explained by Mandal et al. that the lipid shell

enveloping the core of LPHNs is biocompatible and exhibits behavior similar to that of cell membranes, which has higher affinity to the lipid structured cell surface, promote the fusion of the nanocarriers to the cell membrane and deliver drugs more efficiently into the tumor site (Mandal et al., 2013). Considered about the lower toxicity of LPHNs due to the body weight lost test and the data of CRE, WBC and ALT, LPHNs exhibited improved anticancer activity along with lower toxicity than the free drugs.

Conclusions

In the present study, TAB-CIS/5-FU LPHNs were prepared. The LPHNs were stable and able to release drugs in sustained manners. 63.9% of cell uptake was achieved by TAB-CIS/5-FU LPHNs, with the best *in vivo* antitumor ability. The best synergistic effect with the lowest CI value (0.68) was achieved at the ratio of 1/1, which was determined for the dosage of drugs in the LPHNs preparation. TAB-CIS/5-FU LPHNs provides a new strategy for synergistic treating of EAC with higher efficacy and reduced side effects, introducing this system as a candidate for EAC therapy.

Table 2. IC₅₀ and CI₅₀ values of CIS/5-FU LPHNs with different CIS to 5-FU ratios.

Nanoparticles	CIS to 5-FU ratios (w/w)	IC ₅₀ of CIS (μM)	IC ₅₀ of 5-FU (μM)	CI
CIS LPHNs	–	29.3 ± 1.5	–	–
5-FU LPHNs	–	–	31.5 ± 1.8	–
CIS/5-FU LPHNs	5–1	23.9 ± 1.3	4.78 ± 0.5	0.97
CIS/5-FU LPHNs	2–1	18.6 ± 0.8	9.3 ± 0.4	0.93
CIS/5-FU LPHNs	1–1	10.3 ± 1.1	10.3 ± 1.2	0.68
CIS/5-FU LPHNs	1–2	8.6 ± 0.5	17.2 ± 1.7	0.84
CIS/5-FU LPHNs	1–5	5.06 ± 0.4	25.4 ± 1.3	0.98

Values represented as mean ± standard deviation (n = 10).

Table 3. WBC, ALT, and CRE measurements.

Formulation	WBC (K/μL)	ALT (U/L)	CRE (mg/dL)
CIS/5-FU LPHNs	3.5 ± 0.8	13.4 ± 1.3	0.11 ± 0.03
CIS LPHNs	3.1 ± 0.9	14.1 ± 1.5	0.13 ± 0.03
5-FU LPHNs	3.0 ± 0.7	12.9 ± 1.1	0.12 ± 0.02
LPHNs	2.9 ± 0.5	12.5 ± 1.9	0.10 ± 0.03
TAB-CIS/5-FU LPHNs	3.3 ± 0.6	14.1 ± 1.3	0.13 ± 0.04
CIS/5-FU	3.7 ± 0.6	14.4 ± 2.1	0.29 ± 0.05
0.9% saline	2.8 ± 0.3	13.1 ± 1.8	0.11 ± 0.02

Values represented as mean ± standard deviation (n = 10).

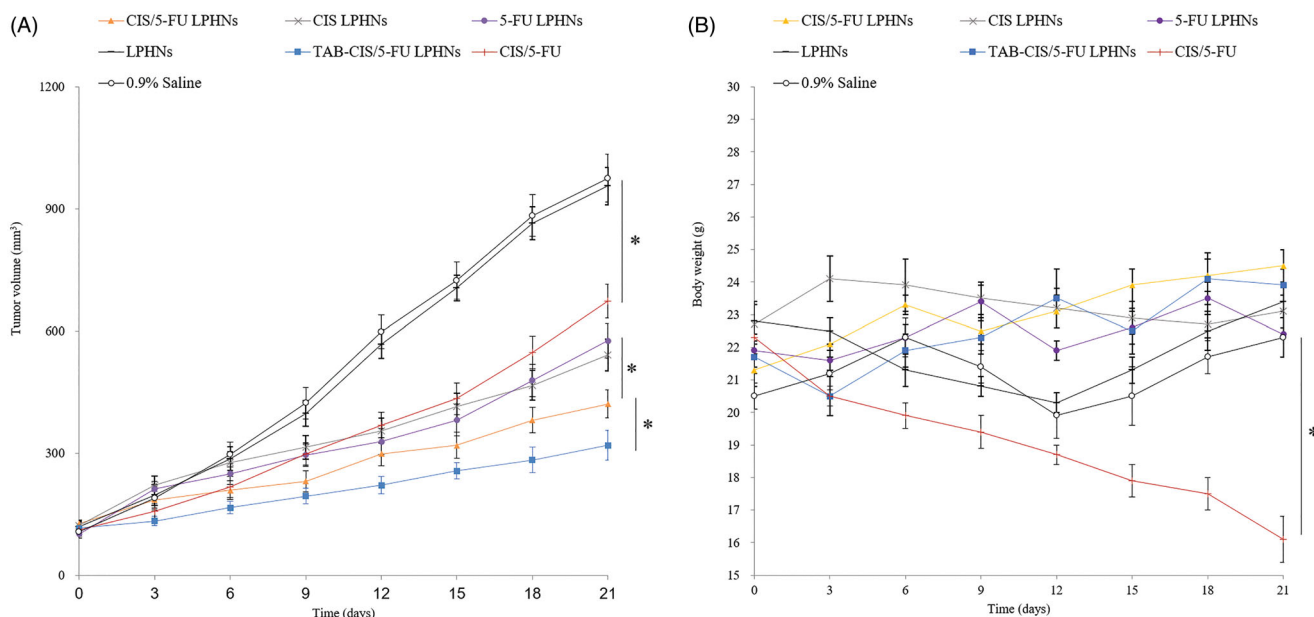


Figure 6. *In vivo* antitumor ability of LPHNs (A) and body weight changes (B). Values represented as mean ± standard deviation (n = 10).

Disclosure statement

No potential conflict of interest was reported by the author(s).

References

- Bang YJ, Van Cutsem E, Feyereislova A, et al. (2010). Trastuzumab in combination with chemotherapy versus chemotherapy alone for treatment of HER2-positive advanced gastric or gastro-oesophageal junction cancer (ToGA): a phase 3, open-label, randomised controlled trial. *Lancet* 376:687–97.
- Bian Y, Guo D. (2020). Targeted therapy for hepatocellular carcinoma: co-delivery of sorafenib and curcumin using lactosylated pH-responsive nanoparticles. *Drug Des Devel Ther* 14:647–59.
- Bosetti C, Levi F, Ferlay J, et al. (2008). Trends in oesophageal cancer incidence and mortality in Europe. *Int J Cancer* 122:1118–29.
- Cao C, Wang Q, Liu Y. (2019). Lung cancer combination therapy: doxorubicin and β -elemene co-loaded, pH-sensitive nanostructured lipid carriers. *Drug Des Devel Ther* 13:1087–98.
- Cedrowska E, Pruszyński M, Gawęda W, et al. (2020). Trastuzumab conjugated superparamagnetic iron oxide nanoparticles labeled with 225Ac as a perspective tool for combined α -radioimmunotherapy and magnetic hyperthermia of HER2-positive breast cancer. *Molecules* 25:1025.
- Chang CH, Liu SY, Chi CW, et al. (2015). External beam radiotherapy synergizes ¹⁸⁸Re-liposome against human esophageal cancer xenograft and modulates ¹⁸⁸Re-liposome pharmacokinetics. *Int J Nanomedicine* 10:3641–9.
- Chou TC, Talalay P. (1983). Analysis of combined drug effects: a new look at a very old problem. *Trends Pharmacol Sci* 4:450–4.
- Chow WH, Finkle WD, McLaughlin JK, et al. (1995). The relation of gastro-oesophageal reflux disease and its treatment to adenocarcinomas of the esophagus and gastric cardia. *JAMA* 274:474–7.
- Cossentino MJ, Wong RK. (2003). Barrett's esophagus and risk of esophageal adenocarcinoma. *Semin Gastrointest Dis* 14:128–35.
- Dassie E, Arcidiacono D, Wasiake I, et al. (2015). Detection of fluorescent organic nanoparticles by confocal laser endomicroscopy in a rat model of Barrett's esophageal adenocarcinoma. *Int J Nanomedicine* 10:6811–23.
- Doi T, Shitara K, Naito Y, et al. (2017). Safety, pharmacokinetics, and anti-tumour activity of trastuzumab deruxtecan (DS-8201), a HER2-targeting antibody-drug conjugate, in patients with advanced breast and gastric or gastro-oesophageal tumours: a phase 1 dose-escalation study. *Lancet Oncol* 18:1512–22.
- Duan W, Liu Y. (2018). Targeted and synergistic therapy for hepatocellular carcinoma: monosaccharide modified lipid nanoparticles for the co-delivery of doxorubicin and sorafenib. *Drug Des Devel Ther* 12:2149–61.
- Fernandes E, Ferreira D, Peixoto A, et al. (2019). Glycoengineered nanoparticles enhance the delivery of 5-fluorouracil and paclitaxel to gastric cancer cells of high metastatic potential. *Int J Pharm* 570:118646.
- Guo S, Zhang Y, Wu Z, et al. (2019). Synergistic combination therapy of lung cancer: cetuximab functionalized nanostructured lipid carriers for the co-delivery of paclitaxel and 5-demethylornibetin. *Biomed Pharmacother* 118:109225.
- Hong Y, Che S, Hui B, et al. (2019). Lung cancer therapy using doxorubicin and curcumin combination: targeted prodrug based, pH sensitive nanomedicine. *Biomed Pharmacother* 112:108614.
- Jemal A, Bray F, Center MM, et al. (2011). Global cancer statistics. *CA Cancer J Clin* 61:69–90.
- Jung HA, Adenis A, Lee J, et al. (2013). Nomogram to predict treatment outcome of fluoropyrimidine/platinum-based chemotherapy in metastatic esophageal squamous cell carcinoma. *Cancer Res Treat* 45:285–94.
- Kim B, Shin J, Wu J, et al. (2020). Engineering peptide-targeted liposomal nanoparticles optimized for improved selectivity for HER2-positive breast cancer cells to achieve enhanced in vivo efficacy. *J Control Release* 322:530–41.
- Li M, Tang Z, Lin J, et al. (2014). Synergistic antitumor effects of doxorubicin-loaded carboxymethyl cellulose nanoparticle in combination with endostar for effective treatment of non-small-cell lung cancer. *Adv Healthc Mater* 3:1877–88.
- Li Y, Gobin AM, Dryden GW, et al. (2013). Infrared light-absorbing gold/gold sulfide nanoparticles induce cell death in esophageal adenocarcinoma. *Int J Nanomedicine* 8:2153–61.
- Lindblad M, Ye W, Lindgren A, Lagergren J. (2006). Disparities in the classification of esophageal and cardia adenocarcinomas and their influence on reported incidence rates. *Ann Surg* 243:479–85.
- Makwana PK, Jethva PN, Roy I. (2011). Coumarin 6 and 1,6-diphenyl-1,3,5-hexatriene (DPH) as fluorescent probes to monitor protein aggregation. *Analyst* 136:2161–7.
- Mandal B, Bhattacharjee H, Mittal N, et al. (2013). Core-shell-type lipid-polymer hybrid nanoparticles as a drug delivery platform. *Nanomedicine* 9:474–91.
- Miao L, Guo S, Zhang J, et al. (2014). Nanoparticles with precise ratio-metric co-loading and co-delivery of gemcitabine monophosphate and cisplatin for treatment of bladder cancer. *Adv Funct Mater* 24:6601–11.
- Moelans CB, van Diest PJ, Milne AN, Offerhaus GJ. (2010). Her-2/neu testing and therapy in gastroesophageal adenocarcinoma. *Patholog Res Int* 2011:674182.
- Mukthavaram R, Jiang P, Saklecha R, et al. (2013). High-efficiency liposomal encapsulation of a tyrosine kinase inhibitor leads to improved in vivo toxicity and tumor response profile. *Int J Nanomedicine* 8:3991–4006.
- Niza E, Noblejas-López MDM, Bravo I, et al. (2019). Trastuzumab-targeted biodegradable nanoparticles for enhanced delivery of dasatinib in HER2+ metastatic breast cancer. *Nanomaterials (Basel)* 9:1793.
- Oh KS, Lee H, Kim JY, et al. (2013). The multilayer nanoparticles formed by layer by layer approach for cancer-targeting therapy. *J Control Release* 165:9–15.
- Pang J, Xing H, Sun Y, et al. (2020). Non-small cell lung cancer combination therapy: hyaluronic acid modified, epidermal growth factor receptor targeted, pH sensitive lipid-polymer hybrid nanoparticles for the delivery of erlotinib plus bevacizumab. *Biomed Pharmacother* 125:109861.
- Pickens A, Orringer MB. (2003). Geographical distribution and racial disparity in esophageal cancer. *Ann Thorac Surg* 76:S1367–S9.
- Pohl H, Welch HG. (2005). The role of overdiagnosis and reclassification in the marked increase of esophageal adenocarcinoma incidence. *J Natl Cancer Inst* 97:142–6.
- Rodallec A, Franco C, Robert S, et al. (2020). Prototyping trastuzumab docetaxel immunoliposomes with a new FCM-based method to quantify optimal antibody density on nanoparticles. *Sci Rep* 10:4147.
- Ruan C, Liu L, Lu Y, et al. (2018). Substance P-modified human serum albumin nanoparticles loaded with paclitaxel for targeted therapy of glioma. *Acta Pharm Sin B* 8:85–96.
- Schoppmann SF, Jesch B, Friedrich J, et al. (2010). Expression of Her-2 in carcinomas of the esophagus. *Am J Surg Pathol* 34:1868–73.
- Siewert JR, Ott K. (2007). Are squamous and adenocarcinomas of the esophagus the same disease? *Semin Radiat Oncol* 17:38–44.
- Silva CO, Rijo P, Molpeceres J, et al. (2015). Polymeric nanoparticles modified with fatty acids encapsulating betamethasone for anti-inflammatory treatment. *Int J Pharm* 493:271–84.
- Soularue É, Cohen R, Tournigand C, et al. (2015). Efficacy and safety of trastuzumab in combination with oxaliplatin and fluorouracil-based chemotherapy for patients with HER2-positive metastatic gastric and gastro-oesophageal junction adenocarcinoma patients: a retrospective study. *Bull Cancer* 102:324–31.
- Thanki K, Zeng X, Foged C. (2019). Preparation, characterization, and in vitro evaluation of lipidoid-polymer hybrid nanoparticles for siRNA delivery to the cytosol. *Methods Mol Biol* 1943:141–52.
- Vaughan TL, Davis S, Kristal A, Thomas DB. (1995). Obesity, alcohol, and tobacco as risk factors for cancers of the esophagus and gastric cardia: adenocarcinoma versus squamous cell carcinoma. *Cancer Epidemiol Biomarkers Prev* 4:85–92.
- Wang H, Agarwal P, Zhao S, et al. (2015). Hyaluronic acid-decorated dual responsive nanoparticles of Pluronic F127, PLGA, and chitosan for targeted co-delivery of doxorubicin and irinotecan to eliminate cancer stem-like cells. *Biomaterials* 72:74–89.

- Wang J, Su G, Yin X, et al. (2019). Non-small cell lung cancer-targeted, redox-sensitive lipid-polymer hybrid nanoparticles for the delivery of a second-generation irreversible epidermal growth factor inhibitor-afatinib: in vitro and in vivo evaluation. *Biomed Pharmacother* 120:109493.
- Yang T, Zhao P, Rong Z, et al. (2016). Anti-tumor efficiency of lipid-coated cisplatin nanoparticles co-loaded with MicroRNA-375. *Theranostics* 6:142-54.
- Ychou M, Boige V, Pignon JP, et al. (2011). Perioperative chemotherapy compared with surgery alone for resectable gastroesophageal adenocarcinoma: an FNCLCC and FFCD multicenter phase III trial. *J Clin Oncol* 29:1715-21.
- Yu W, Liu C, Liu Y, et al. (2010). Mannan-modified solid lipid nanoparticles for targeted gene delivery to alveolar macrophages. *Pharm Res* 27:1584-96.
- Zhang R, Ru Y, Gao Y, et al. (2017). Layer-by-layer nanoparticles co-loading gemcitabine and platinum (IV) prodrugs for synergistic combination therapy of lung cancer. *Drug Des Devel Ther* 11: 2631-42.